Depth-Resolved Holography Through Turbid Media Using Photorefraction

Sam C. W. Hyde, Richard Jones, Nick P. Barry, J. C. Dainty, *Member, IEEE*, Paul M. W. French, K. M. Kwolek, David D. Nolte, and M. R. Melloch, *Senior Member, IEEE*

(Invited Paper)

***Abstract*— A technique based on photorefractive holography for imaging objects obscured by a scattering medium is presented. Using ultrashort pulse illumination, depth-resolved whole-field images of three-dimensional objects embedded in scattering media have been obtained. Bulk photorefractive crystals and photorefractive multiple quantum-well (MQW) devices have been investigated as the hologram recording element. Images have been obtained through media of up to 16 scattering mean free paths with a system based on bulk rhodium-doped barium titanate (Rh:$BaTiO_3$). Using MQW devices, a real-time image acquisition ($<$0.4 ms) has been demonstrated when imaging through eight scattering mean free paths. The relative merits of photorefractive holography are discussed, including its potential to provide a higher dynamic range of detection than traditional photographic film based or electronic holography. This could be important for *in vivo* imaging through biological tissue.**

I. Introduction

NEAR-INFRARED radiation offers the potential for medical diagnostic and functional imaging in biological tissue since the absorption of typical biological tissue in this spectral region is at a minimum. The use of optical radiation, rather than X-rays or ultrasound, provides the opportunity to make spectroscopic measurements in biological tissue that can be of significant diagnostic value. Furthermore, this spectral window overlaps the tuning ranges of semiconductor laser diodes, Ti:sapphire lasers, and diode-pumped Cr:LiSAF lasers [1], which makes near infrared laser-based instrumentation viable. At these wavelengths, however, biological tissue exhibits a high scattering cross section that usually results in severe image degradation due to multiple scattering. Much research has focused on methods to recover the image information in the presence of this scattered light. In particular, various schemes have been devised to form images using ballistic (unscattered) light that is normally obscured by the diffuse background noise. These include spatial filtering, e.g., [2], confocal imaging, e.g., [3], time gating, e.g., [4]–[6] and coherence gating, e.g., [7], [8], and polarization gating, e.g., [9]. When imaging with a reflection geometry, i.e., using back-scattered light, time-gating can also provide depth-resolved (time-of-flight) image information that may be used to reconstruct three-dimensional (3-D) images. Time-gating may be realized using an incoherent time-resolved detector [4], a nonlinear optical time-of-flight gate, e.g., [5], [6], and [10], or by low-coherence interferometry, e.g., [11]. It should be noted that all systems that form images through turbid media using the unscattered ballistic light are inherently limited to small scattering (tissue) depths since ballistic signals suffer exponential attenuation on passage through the scattering media. Hee *et al.* [11] estimated that for reasonable powers of tissue irradiation in the infrared, the unscattered ballistic component of the light will be reduced to the shot noise detection limit after propagating through approximately 36 scattering mean free paths (mfp) of a scattering medium. This corresponds to a "typical" tissue thickness of $\sim$4 mm ($\sim$2 mm tissue depth for reflection geometrys) and is potentially useful for clinically relevant applications such as skin cancer screening, diagnosing and/or monitoring other dermatological conditions, imaging of the eye, and endoscope-based imaging systems.

In order to assess and compare the performance of different ballistic light imaging systems, it is useful to establish criteria by which to evaluate them. We identify the four most important criteria as: 1) *resolution* (transverse spatial resolution and longitudinal resolution for depth-resolved imaging systems); 2) *sensitivity* (i.e., the minimum power level of ballistic light required to record an image); 3) *dynamic range* (i.e., the maximum usable ratio of background scattered light to ballistic signal light); and 4) *image acquisition time* (i.e., the time needed to acquire the data necessary to construct a full two- or three-dimensional image). Different imaging systems may have different advantages and tradeoffs between the criteria listed above. For example, in the case of confocal scanning microscopy, the transverse resolution can be extremely high but, since the total image information is obtained by scanning source and detector pixel by pixel, increasing the image resolution comes at the expense of an increased acquisition time and subsequently a lower frame rate. It is possible to achieve high sensitivity with a ballistic imaging system and approach the quantum limit for detection but only if one uses a sufficiently long integration time. The dynamic range of a ballistic imaging system can be limited by the photodetector,

Manuscript received October 1, 1996. This work was supported by the U.K. Engineering and Physical Sciences Research Council (EPSRC). The work of S. C. W. Hyde was supported by an EPSRC Cooperative Award in Science and Engineering studentship supported by Kodak Ltd. The work of R. Jones was supported by an EPSRC studentship.

S. C. W. Hyde, R. Jones, N. P. Barry, and J. C. Dainty are with the Femtosecond Optics Group, Physics Department, Imperial College of Science, Technology and Medicine, London SW7 2BZ, U.K.

K. M. Kwolek and D. D. Nolte are with the Department of Physics, Purdue University West Lafayette, IN 47907-1396 USA.

M. R. Melloch is with the School of Engineering, Purdue University West Lafayette, IN 47907-1396 USA.

Publisher Item Identifier S 1077-260X(96)09602-5.

which will usually be saturated by the diffuse background unless some means is employed to block the scattered light. This may be partially achieved by a spatial filter that will reject light, which is scattered off-axis, but there will be a tradeoff between scattered light rejection and achievable spatial resolution for two-dimensional (2-D) imaging systems. It should be understood that it is necessary to consider the required performance of an imaging system for a specific application, in order to select the most promising technology. The work reported here has been motivated by a desire to develop imaging systems for *in vivo* applications such as screening for skin cancer, for which rapid image acquisition time is a priority. To this end we have concentrated on developing "whole-field" imaging techniques, which acquire all the pixel information in parallel, thereby accepting compromises in achievable resolution and sensitivity compared to confocal scanning techniques.

The imaging technique presented in this paper uses holography in photorefractive media [12] as a means of discriminating in favor of the unscattered light that retains coherence with a reference beam. This is related to coherence gating techniques previously reported by various groups including optical heterodyne detection [13] and optical coherence tomography (OCT) [14], as well as to conventional, electronic and light-in-flight holography [8], [15], [16]. It fundamentally differs from other techniques, however, in that this coherent detection system is, to first order, insensitive to the incoherent diffuse light background that does not saturate the detector and therefore does not degrade the dynamic range of the coherent detection. (This is in contrast to electronic holography and other techniques that record the total intensity distribution due to both ballistic and scattered light and then extract the coherent component.) The implementation of our technique also differs from many of the previously reported coherent imaging systems in that it is a whole-field imaging technique, i.e., it acquires a whole 2-D image field in a single acquisition, rather than scanning pixel by pixel, which can result in extremely short image acquisition times. These images are acquired using back-scattered light in a time-gated reflection geometry based on low coherence interferometry and so may be used to reconstruct 3-D images. The use of reusable photorefractive holographic media, such as bulk rhodium-doped barium titanate (Rh:$BaTiO_3$) crystals or photorefractive multiple quantum-well (MQW) devices, allows for fast holographic image recording and the potential for real-time read-out using a third reconstruction beam, which may be adjusted independently to those writing the hologram and so be optimized for detection by a charge-coupled device (CCD) camera.

II. Experiments

A. Photorefractive Imaging Through Turbid Media

The same basic experimental arrangement, which is shown in Fig. 1, was used for photorefractive holography with both Rh:$BaTiO_3$ and MQW recording media. It consisted of a modified Mach–Zender interferometer with the two arms, representing object and reference beams respectively, being recombined at the holographic recording medium. In order to write a hologram, the lengths of the two arms needed to be matched to within a coherence length of the laser. The laser source was a Ti:sapphire laser, which was tunable over the range 720–900 nm and could be operated continuous-wave (CW) or mode-locked to generate pulses of ~100 fs duration at a repetition rate of 80 MHz. For our first experiments with the Rh:$BaTiO_3$ crystal (supplied by Hughes Laboratories), the Ti:sapphire laser was operated CW in order to demonstrate the capability of photorefractive holography to image 2-D objects obscured by scattering media. This had previously been demonstrated by Mamaev *et al.* [12] using an argon ion laser.

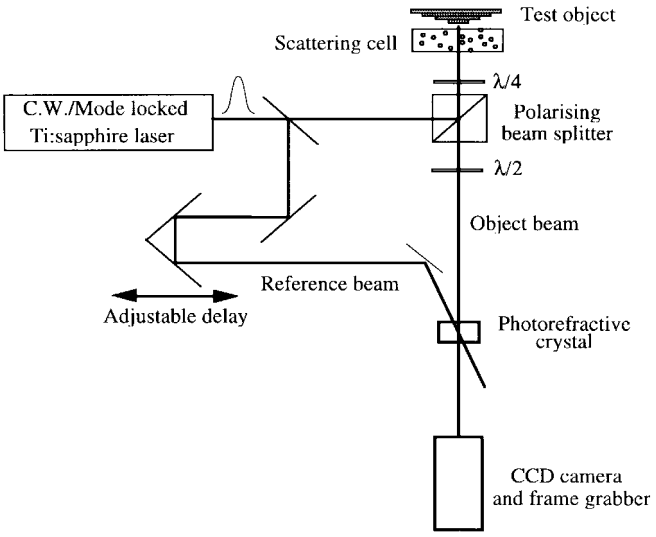

Fig. 1. Experimental configuration for holographic imaging through a scattering medium using a bulk Rh:$BaTiO_3$ crystal.

A USAF test chart was imaged in reflection through a scattering cell that contained a 0.3% water solution of 0.46-μm polystyrene spheres. Mie theory [17] predicts this solution to correspond to approximately 8-mfp scattering depth in the double pass. The incident illumination beam and back reflected object beam were separated using a polarizing beam splitter (PBS) and quarter-wave plate $(\lambda/4)$ combination. After reflection at the PBS, the polarization of the object beam was rotated back to the horizontal (such that it was the same as the reference beam) and relayed onto the CCD camera through the 100-mm focal length lenses $L1$ and $L2$. This lens pair constituted a 4-F imaging system. The Rh:$BaTiO_3$ crystal was located at or near the Fourier plane between the lenses $L1$ and $L2$ and was used to record the hologram that was written when the reference beam was interfered with the object beam at an angle of 70°. Once recorded, the hologram was reconstructed by blocking the object beam and allowing the reference beam to diffract off the hologram, thereby producing an image of the object at the CCD camera. The images recorded on the CCD camera were then captured and stored on computer.

Fig. 2(a) shows the image of the test chart when viewed directly through the scattering medium by the CCD camera. The image was totally obscured by the scattered light. Fig. 2(b) shows the image of the object when viewed through the scattering medium in the imaging system shown in Fig. 1, but without the holographic reconstruction. This demonstrates the ability of spatial filtering to remove some of the scattering

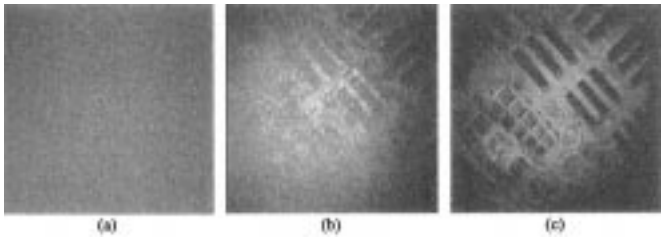

Fig. 2. Holographic image of a test chart recorded when (a) viewed directly through the scattering cell by the CCD camera, (b) viewed through the spatial filter of the imaging setup, and (c) using photorefractive holography in the Rh:$BaTiO_3$ crystal.

light. In this case the spatial filtering was due to the limited collection angle of the lenses and the finite diameter of the Rh:$BaTiO_3$ crystal. With this low degree of filtering it was possible to recover images of the 1 mm wide bars. Fig. 2(c) shows the image of the test chart obtained when the hologram recorded in the Rh:$BaTiO_3$ crystal was read out using the reference beam with the object blocked. This demonstrates the ability of photorefractive holography to reject the scattered light without the compromised resolution of higher degrees of spatial filtering. The smallest observable bars were of 30-μm width. The achievable spatial resolution was limited only by the finite apertures of the optical components in our experimental setup. This experiment clearly demonstrates the ability of photorefractive holography to discriminate against the incoherent background light—*even for CW holography with no time-gating*. The scattered photons reaching the photorefractive crystal did not saturate the response or write "noise" holograms so as to obscure the signal. This is because photorefractive media like Rh:$BaTiO_3$ crystal do not respond to uniform illuminating light fields: *photorefractive media respond to the spatial gradients of intensity distributions*, rather than to the intensity itself [18]. The photons that were scattered in the solution of polystyrene spheres acquired random time-varying Doppler frequency shifts and propagation delays, which meant that during the integration time of the Rh:$BaTiO_3$ crystal, they constituted a (time-averaged) incoherent uniform background. It is important to understand that this phenomenon occurs because dynamic (e.g., liquid) phantoms are used as scattering media and that all coherence-gated imaging techniques, including electronic holography or heterodyne detection, will be able to discriminate against this time-averaged incoherent background. What is specific to photorefractive holography is that the extraction of the coherent image takes place at the photorefractive crystal, which has a huge dynamic range compared to a CCD camera or photodiode. In this experiment, had the scattered light reached reached the simple low-cost CCD camera (which had a measured bit-depth of only $\sim$4), saturation would have prevented an extraction of the coherent image. At the photorefractive crystal, however, these beams were many orders of magnitude too small to prevent the hologram being recorded and reconstructed.

As discussed above, coherent imaging techniques discriminate against scattered light that decorrelates faster than the image acquisition time. This has been demonstrated in many laboratories where liquid scattering phantoms are used owing to the ease with which their optical absorption and scattering properties may be calibrated or calculated. In order to compare our results against other published work, we have adopted the same practice. It should be borne in mind, however, that for many biomedical applications of optical imaging it is necessary to image through relatively stationary scatterers (e.g., tissue). This is a much more difficult challenge, which can in part be addressed by a *time-gated* coherent detection, which uses short coherence length light to provide an ultrafast time gate, thereby rejecting late arriving scattered light that arrives outside the pulse width. This technique is most effective in transillumination systems where there is no scattered light arriving before the ballistic light [19]. It is desirable, however, to use a time-gate in a retro-reflection geometry that can provide depth-resolved 3-D images by using the time of flight information. This is possible using a low-coherence source and works reasonably well when combined with confocal scanning [14], which rejects most of the scattered light by spatial filtering. It is more difficult with whole-field imaging techniques, however, because cross-talk can occur between adjacent pixels where weakly scattered photons interfere, resulting in competing holograms (or speckle). This problem is partially alleviated by spatial averaging across the image field and may be reduced by minimizing the coherence length or by introducing spatial incoherence across the image field e.g., [20]. Note that incoherent time-gated whole-field imaging techniques also suffer image degradation from cross-talk and, unlike coherent techniques, do not reject any of the scattered light that arrives within the detection time window. The future application of all ballistic imaging techniques to biomedicine will be greatly impacted by the degree to which the problem of cross-talk is overcome.

B. Time-of-Flight Holography for Depth Resolution

Time-gated holography, known as light-in-flight holography, was first proposed by Abramson [15] and later applied to biomedical imaging by Spears *et al.* [21]. We first demonstrated the use of light-in-flight holography to obtain depth-resolved images through 8 mfp of scattering medium, with a depth resolution of 2 mm [22]. The imaging setup for depth-resolved holography was as shown in Fig. 1, with a mode-locked Ti:sapphire laser producing 3-ps pulses used as the source. The imaging system, shown in Fig. 3, was similar to the CW system described above, except that holograms could only be written when the interferometer arm lengths were matched to within the coherence length of the source ($\sim$1 mm). This therefore provided depth resolution. It is interesting to note that ultrashort pulse mode-locked lasers are not strictly needed for this application since the optical source need only have a short coherence length (i.e., broad spectral bandwidth) to achieve the time-of-flight-gating and hence the depth resolution. In principle, any broad-band radiation source could be used, but in practice, when imaging through turbid media that strongly attenuate the ballistic signal, mode-locked lasers are the most convenient source of high-power broad bandwidth light.

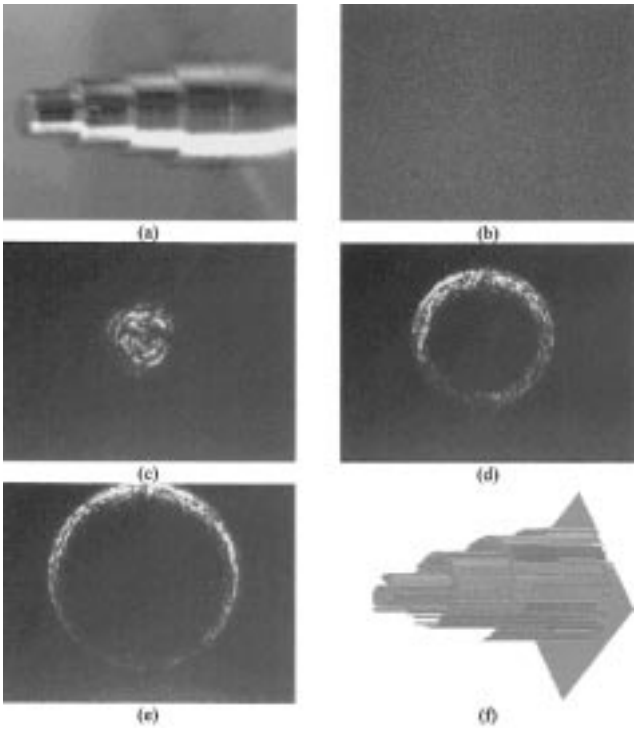

Fig. 3. Depth-resolved holographic images showing (a) picture of the 3-D test object, (b) image of test object when viewed directly through 8 mfp of scattering medium, (c)–(e) picosecond depth-resolved images of each of the top three layers, (f) 3-D computer rendering of depth-resolved images.

An object, consisting of a series of concentric aluminum cylinders, ranging from 2 to 5 mm in diameter and separated in depth by 1 mm, was used "end-on" as the 3-D test object in our first experiment to demonstrate depth-resolved imaging through a turbid medium [this object is shown in Fig. 3(a)]. The image obtained directly through 8 mfp of scattering medium is shown in Fig. 3(b), and as can be seen, no significant image can be recognized. Fig. 3(c)–(e) show the depth-resolved images obtained through the scattering medium by photorefractive holography. For each image acquisition, the delay of the reference arm was adjusted such that the reference beam pulse arrived at the crystal at the same time as light back-scattered from the particular layer of interest in the object. The power incident on the sample was approximately 500 mW over a 4-mm-diameter area (an intensity of $\sim$ 2.5 W/cm^2) and the reference beam power was approximately 20 mW. By varying the delay of the reference arm between each acquisition, a set of images sufficient to reconstruct a 3-D image of the object could be obtained. Each depth-resolved image was recorded in approximately 1 s and then transferred to the computer for rendering. A 3-D computer reconstruction of the object as seen through 8 mfp is shown in Fig. 3(f). The depth resolution of the images was $\sim$2 mm, while the transverse spatial resolution was approximately 30 μm. This experiment thus confirmed that photorefractive holography could be used for depth-resolved imaging through turbid media, although the performance of this first experimental apparatus was far from what is required for practical application. We have subsequently endeavored to evaluate our ballistic imaging technique using the criteria discussed above to establish its potential limits and to optimize our system accordingly. The results of this work are discussed in the next four sections.

C. Spatial Resolution

The first general consideration of a 3-D imaging system is the achievable transverse and longitudinal spatial resolution. Although for many biomedical imaging applications detectability, rather than absolute resolution, is the key issue, spatial resolution is still a useful parameter in that it provides a means to compare different techniques and it gives an indication of the smallest heterogeneity likely to be detected. In the initial experiments described above, a transverse resolution of 30 μm was demonstrated, which was limited by the apertures of the optical components used, but the depth resolution was of $\sim$1 mm. For on-axis holography (i.e., when the reference and object beam are exactly collinear) the depth resolution is determined purely by the coherence length of the optical source. However, for a noncollinear writing beam geometry, as used in these experiments, the realizable depth resolution is governed also by geometric considerations, which we shall refer to as "walkoff" [22].

For low-coherence light, for which the coherence length is significantly smaller that the transverse dimensions of the beams, the angle of incidence between the beams causes a variation in arrival time of the reference pulse laterally across the holographic medium and therefore with respect to the arriving image signal. Thus the reconstructed hologram will contain information from an extended depth within the object determined by the interaction angle of the writing beams, as shown in Fig. 4. This effect can compromise both the transverse spatial and longitudinal depth resolution. Ideally, it should be minimized by reducing the angle between writing beams to approach a collinear beam geometry. This implies that a large period grating ($\Lambda_g \geq 10$ μm) will be written in the recording medium (according to the Bragg equation, $\Lambda_g = \lambda/2\sin\theta$, where θ is the half angle between writing beams). The systems described above operated in the diffusion regime of the photorefractive effect (i.e., with no externally applied electric field). In this regime the space charge field, and hence diffraction efficiency of the refractive index grating, is greatly reduced for long grating periods compared to the optimum grating period, which is typically of the order of 1 μm. Fig. 5 shows how the two beam coupling gain varies with grating spacing for the two types of Rh:$BaTiO_3$ used, (for weakly modulated beams, the diffraction efficiency varies as the square of the two beam coupling gain [23]). One route to addressing this problem is to use a 45°-cut crystal [24]. This gives better access to the largest electrooptic coefficient in Rh:$BaTiO_3$ and allows smaller writing angles to be used than would be possible with the 0°-cut crystal. It is possible to estimate the achievable depth resolution from geometrical analysis of the interaction angles and coherence lengths. In practice, a compromise is reached between the average grating period (hence the grating diffraction efficiency and overall system "sensitivity") and the achievable depth resolution [25]. Using an experimental setup similar to that shown in Fig. 1, but with a 100-fs femtosecond Ti:sapphire laser source at

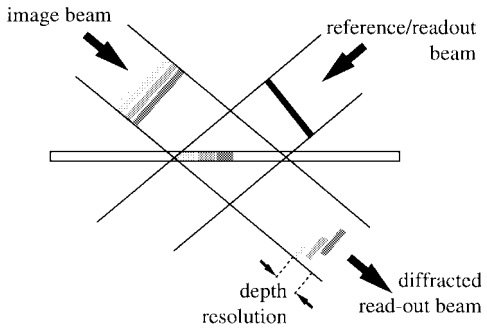

Fig. 4. Diagram illustrating the problem of "walkoff" in the holographic when not using a collinear writing beam geometry.

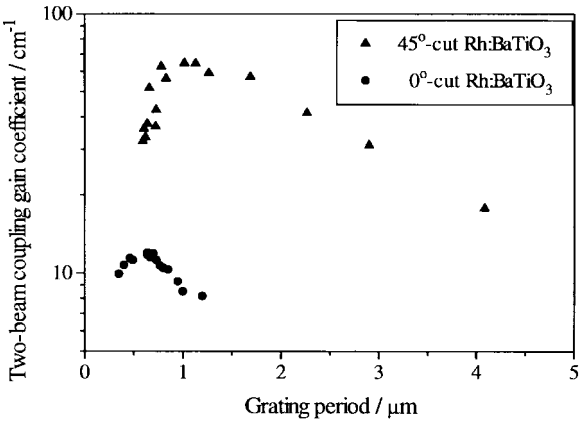

Fig. 5. Two beam coupling gain coefficient as a function of grating period (Λ_G) for 0°-cut and 45°-cut Rh:$BaTiO_3$ crystals.

790 nm, an angle of $\sim 6^\circ$ between the beams, and a 45°-cut Rh:$BaTiO_3$ photorefractive crystal, a depth and transverse spatial resolution of 100 μm have been achieved [25].

D. Sensitivity

We have defined sensitivity as the weakest intensity ballistic signal with which it is possible to record a useful hologram. This directly limits the maximum thickness of scattering medium through which it is possible to image, although a more severe limit may be imposed by the tolerance to scattered light (i.e., the dynamic range). For the photorefractive imaging system, the tradeoff between sensitivity and depth-resolution, due to the properties of the photorefractive medium, has already been discussed. Once a minimum performance (e.g., 100-μm depth and transverse resolution) is determined, the beam geometry and grating period are fixed and one must optimize the sensitivity with other parameters of the system. An attractive feature of our technique is that the holograms are reconstructed using a read-out beam that may be of almost arbitrary intensity: even very weak holograms with a diffraction efficiency of 10^{-9} will diffract sufficient light from a 100-mW read-out beam to relay an image to our low-cost CCD camera. This figure may be further reduced by employing a more powerful read-out laser beam or a more sensitive, e.g., cooled, CCD camera. Eventually, the minimum diffraction efficiency (and therefore hologram modulation depth) required is set by the optical quality of the photorefractive medium in which inhomogeneities may scatter the read-out beam into the CCD camera and saturate it. To some extent (limited by the bit-depth of the camera) this static noise signal can be removed by image subtraction and can also be reduced by spatial filtering of the reconstructed image. Beam fanning may also present a problem at extremely large read-out beam intensities. There are other factors that also set an upper limit on the read-out beam intensity, some of which are briefly discussed below.

Once the optical quality of the photorefractive medium and the camera bit-depth have set the minimum holographic diffraction efficiency required, the next consideration is the relative intensity of the signal and reference beams when recording the hologram. This beam ratio determines the modulation depth of the fringe pattern and hence the diffraction efficiency. The total average intensity in the beams determines the response time of the system, i.e., the time taken for the grating being written in the photorefractive medium to reach its maximum steady-state value (the response time is inversely proportional to the average incident intensity). While using equal intensities in the signal and reference beams will maximize the modulation depth, the low intensity of typical ballistic signals encountered when imaging through scattering media will mean that the response time becomes unacceptably long e.g., hours. The response time must be reduced such that the image acquisition time is compatible with practical applications. This may be achieved by increasing the intensity of the reference beam—at the cost of reduced modulation depth (and therefore reduced diffraction efficiency).

To determine the optimum levels for the various beams, the holographic imaging system was investigated (in the absence of a scattering medium) to determine the minimum ballistic light intensity required to record and read-out a hologram, as a function of the ratios between the different beams. The imaging system used is shown in Fig. 6 and was based on the setup described previously. The image beam passed through a series of 4F image relay lens pairs (focal length = 75 mm) forming three Fourier planes. The first Fourier plane was not exploited in this experiment. The photorefractive crystal was located at the second Fourier plane and the third Fourier plane contained a 0.3-mm pinhole employed as a spatial filter. This arrangement, which permitted the detection of very weak diffracted beams (although no image information), was used in order to decouple the holographic recording process from the scattering noise encountered when reading out the hologram. With the read-out beam maintained at 36 mW/cm^2, the minimum signal beam intensity required to record an observable hologram was measured for various reference beam intensities. The experiment was performed with integration times of both 1 min and 5 min. The results for 5-min integration are shown in Fig. 7(a). This indicates that the minimum signal intensity with which it was possible to record a usable hologram was $\sim$10 nW/cm^2 for the 5-min integration time. Similarly, a value of 100 nW/cm^2 was obtained for the 1-min integration time. These minimum figures were obtained for reference beam powers of $\sim$40 mW/cm^2.

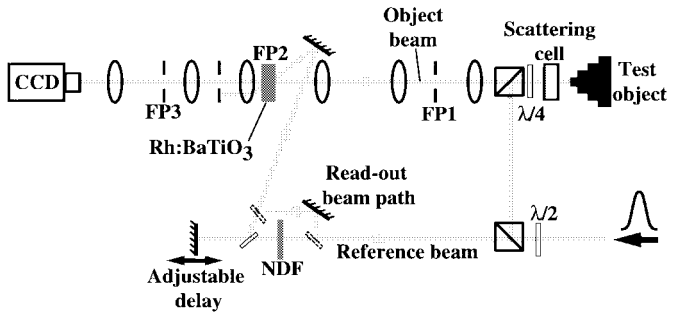

Fig. 6. Experiment configuration used to investigate sensitivity of the holographic imaging system. The dashed line marks the path of the beam used to read out the hologram once the reference and object beam had been blocked. Abbreviations refer to FP: Fourier plane. NDF: Neutral density filter; BS: Beam splitter; PBS: Polarizing beam splitter; $\lambda/2$: Half-wave plate; $\lambda/4$: Quarter-wave plate.

To optimize the intensity of the read-out beam, a similar experiment was performed with the reference beam kept constant and minimum signal required to record a hologram being measured for various read-out beam intensities. The integration time used for this experiment was 1 min, and the variation of minimum ballistic signal intensity as a function of read-out beam intensity is shown in Fig. 7(b). As expected, this shows a decrease in the minimum signal detectable with increased read-out intensity, which corresponds to an increased sensitivity. Above 200 mW/cm^2, however, the marginal improvement in sensitivity for increasing read-out power is relatively small. This was probably due to some of the scattered read-out noise passing through the spatial filter and reaching the CCD camera to obscure the holographic reconstruction. A second factor was the increased rate of erasure: at high read-out beam intensities, the uniform reference beam illumination will erase the image stored in the photorefractive crystal. There will be no advantage in increasing the read-out beam intensity beyond that value that erases the hologram in a time comparable to the integration time of the CCD camera.

Following this study of the optimum ratios of beam intensities, the experimental system represented in Fig. 6 was used for depth-resolved imaging through a scattering cell. First, a holographic image of the USAF test chart was obtained through 16 mfp of scattering solution. The direct image of the test chart through the imaging system, as seen at the CCD camera when there was no scatterer present is shown in Fig. 8(a). The reduced definition of the bar patterns is a consequence of the spatial filters used in this experiment. A holographic image of the test chart acquired through 16 mfp of scattering medium is shown in Fig. 8(b). This clearly shows the 100-μm bars of the test chart. The integration time for the holographic recording of the image obscured behind 16 mfp was $\sim$ 5 min. Translating the test chart longitudinally established that the depth resolution was 100 μm, as predicted from the pulse duration and beam geometry.

The depth resolution was also demonstrated using a 3-D test object that consisted of a set of cylindrical steps with diameters ranging from 1 to 5 mm in 1-mm increments, which were separated in depth by 100 μm. This object was unpolished and provided no significant specular reflection, but

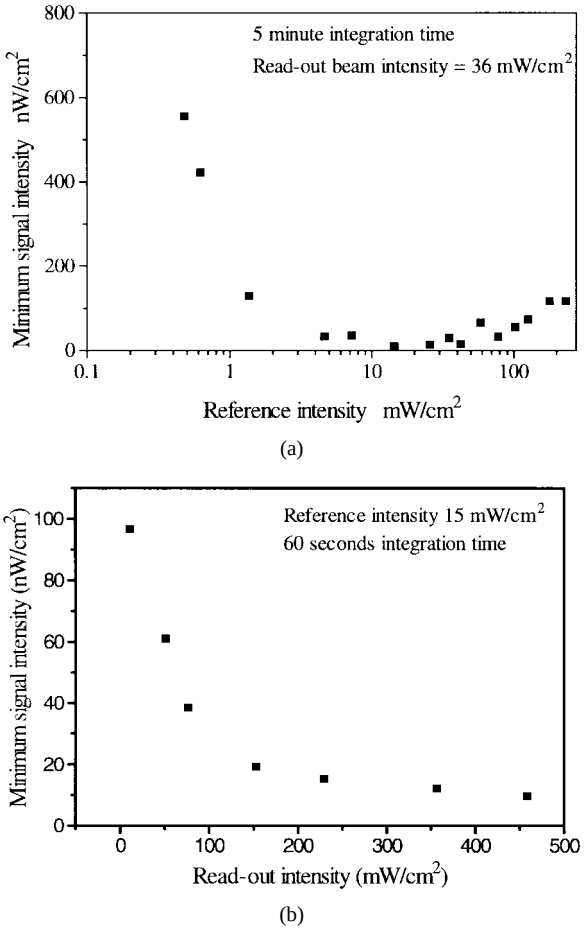

Fig. 7. Minimum incident signal intensity to record and reconstruct a hologram in the Rh:$BaTiO_3$ as a function of (a) reference beam intensity and (b) read-out beam intensity.

back-scattered $\sim$8% of the incident light. A depth-resolved image of each of the layers of the test object was acquired, as outlined previously, and the whole field images were computer rendered to produce a reconstruction of the 3-D object. In the absence of the scattering medium, individual depth-resolved images required an integration time of approximately 1 s. When obscured by a scattering solution of 14-mfp scattering depth, the integration time required was of the order of 5 min for an incident intensity of 0.65 W/cm^2 at the scattering cell. Fig. 9(a) shows a reconstruction from a series of holographic images acquired in the absence of the scattering medium. Fig. 9(b) and (c) shows reconstructed holographic images when the test chart was obscured by 12 mfp and 14 mfp (in double pass) of scattering solution, respectively. Although there is a slight degradation in the image quality at the greater scattering depth, the depth resolution of the individual holographic images that make up the 3-D rendering did not appear to be compromised.

E. Dynamic Range

The dynamic range of ballistic imaging systems can be defined as the maximum sustainable ratio of noise to signal, which still permits an acceptable image to be acquired. Given the use of balanced detection circuits, e.g., [7] and

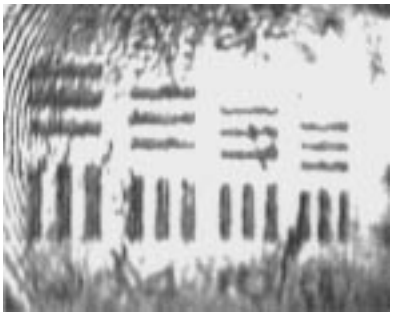

(a)

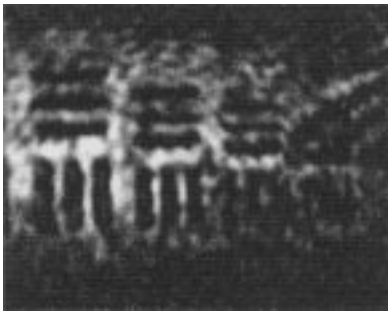

(b)

Fig. 8. Image of test-chart (a) viewed without obscuring scattering medium and (b) recorded through 16 mfp of scattering medium.

(a) (b) (c)

Fig. 9. Computer reconstructions of images of 3-D objects recorded using depth-resolved holographic imaging in Rh:$BaTiO_3$. Images recorded through scattering medium of (a) zero, (b) 12-mfp, (c) 14-mfp scattering depths.

cooled CCD cameras e.g., [19] etc., the major source of noise is that arising from scattered light—the magnitude of which increases with scattering depth. As discussed in the introduction, the Rh:$BaTiO_3$ photorefractive medium was not expected to respond to the uniform illumination fields resulting from the time-averaged scattered light (unlike an incoherent detector such as a photographic film, a CCD camera, or a photodiode). Thus, the ratio of incoherent scattered light to ballistic signal light, which the photorefractive holography can tolerate, is expected to be much greater than for e.g., electronic holography. Consider, for example, the case of electronic holography using an advanced CCD camera system with a dynamic range of 16 b (corresponding to 65 536 gray-scale levels). If all other sources of noise are neglected, once the scattered light reaching the CCD camera becomes 65 536 (or e^{11}) times greater than the ballistic light, it is no longer possible to extract the coherent image because it has less than one gray-scale of intensity. This problem is fundamental to all electronic acquisition techniques that detect the scattered light together with the ballistic light before subtracting it. It may be partially circumvented by using a strong spatial filter to prevent much of the scattered light reaching the CCD camera—albeit at the expense of achievable transverse spatial resolution. Photorefractive holography is different because the "subtraction" is performed optically inside the photorefractive crystal. The incoherent scattered light does not contribute the hologram, and so only the ballistic light writes a hologram that diffracts light into the CCD camera at the electronic detection stage. (Note that all the work reported here was undertaken with a standard CCD camera with a measured bit depth of $\sim$4).

It is clearly interesting to consider the dynamic range of the photorefractive holography technique. In the work with Rh:$BaTiO_3$ described above, holograms with intensities as low as 10 nW/cm^2 were recorded with reference beams of up to 40 mW/cm^2. This demonstrated a minimum dynamic range of 4×10^6. The resulting modulation depth was very low (but still sufficient to provide a useful hologram), and the remaining dc component of the field writing the hologram can be envisaged as a noise source, which did not prevent the recording of the hologram because it was spatially uniform. One can therefore infer that a dynamic range higher than $\sim10^7$ is possible with photorefractive holography. To support this assertion, an experiment was performed with Rh:$BaTiO_3$ using the experimental setup depicted in Fig. 6. The aim was to vary the depth of scattering medium through which the USAF test-chart was imaged and observe the minimum ballistic signal required to form a hologram against an increasing background of scattered light incident on the photorefractive crystal.

For these experiments, a weak 1.6-mm-diameter spatial filter at was employed at the first Fourier plane (FP1) to block the surface reflections from various optical components. This did not significantly reduce the amount of scattered light reaching the photorefractive crystal. The second spatial filter, located at FP3, was 0.6-mm diameter and reduced the scattered light from inhomogeneities within the Rh:$BaTiO_3$ crystal that reached the CCD camera. The intensity in the reference beam was set to $\sim$15 mW/cm^2 and holograms were recorded with an integration time of 5 min. The concentration of the scattering suspension was progressively increased in order to adjust the scattering depth and the minimum incident ballistic power required to write a hologram was determined. This is plotted in Fig. 10(a) as a function of scattering depth in units of mean free paths. Since the ballistic component of the incident light was attenuated by an exponential power factor equal to the number of scattering mean free paths, it was possible to estimate the amount of unscattered ballistic light that was incident at the photorefractive Rh:$BaTiO_3$ crystal. This is plotted as a function of scattering depth in Fig. 12(b), which indicates that the minimum ballistic component required to write a hologram lies within a small range (less than 0.5 nW) and does not appear to increase significantly for increasing scattering depth (N.B. the error bars at low scattering depth are due to the uncertainty of measuring the concentration of the scattering solution). This flat response confirms that, at least for scattering depths up to 16 mfp, the scattered light does not significantly affect the holographic recording process. This is not surprising because, while the scattered light intensity may be very much larger than the intensity of the ballistic

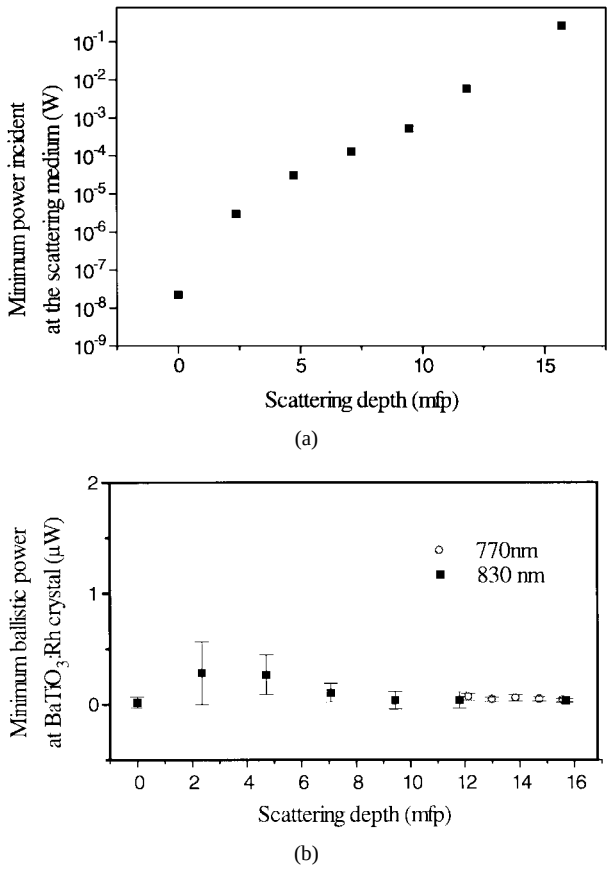

Fig. 10. Minimum (a) incident intensity required to record a hologram of a test-chart obscured behind a scattering medium, using a Rh:$BaTiO_3$ based imaging system, as a function of the thickness of the scattering medium and (b) calculated ballistic power incident on the crystal.

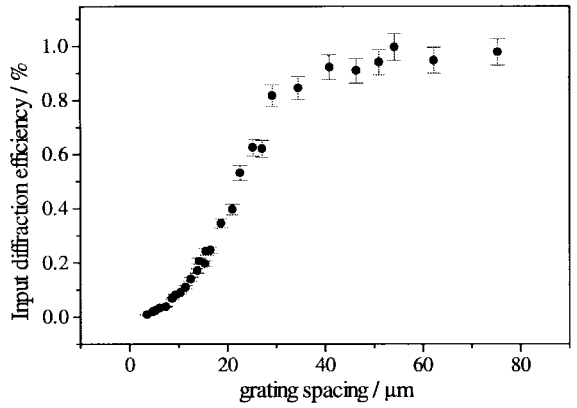

Fig. 11. First-order diffraction efficiency as a function of grating period for a MQW device used in the Franz–Keldysh geometry.

component, it will be smaller than the reference beam and therefore will not significantly change the parameters of the photorefractive recording process (i.e., the modulation depth of the coherent signal).

F. Acquisition Time

The above experiments demonstrate the ability of photorefractive imaging systems to sensitively detect images through reasonably highly scattering materials with a sub-100-μm spatial resolution. However, the sensitivity demonstrated above is at the cost of a long image acquisition time. While photorefractive holography is an intrinsically whole field imaging system, and as such should provide faster image acquisition than confocal scanning systems, the integration times reported here are much too long to be clinically viable. There are, however, alternative photorefractive materials that provide a faster response without forfeiting sensitivity. In addition to Rh:$BaTiO_3$, we have investigated the use of semi-insulating GaAs–AlGaAs MQW devices as the photorefractive recording medium [26]. MQW devices have been shown to have many advantageous nonlinear optical properties in contrast to the bulk semiconductors from which they are grown [27]. In particular, MQW structures give rise to strong, narrow excitonic absorption features whose spectral profile may be changed by an applied electric field, this in turn leads to large electroabsorbtive and electrorefractive nonlinearity's with a typically submillisecond response time. These optical nonlinearity's are due either to the Franz–Keldysh (or field broadening) effect [28] when an electric field is applied parallel to the wells, or to the quantum confined stark effect [29] when a perpendicular electric field is applied. When used as holographic media, semi-insulating MQW devices exhibit a sensitive photorefractive response which provides very high diffraction efficiencies with a sub-ms response time. In addition, due to the applied field the MQW devices work in the drift photorefractive regime and this results in their diffraction efficiency saturating with increased grating period as shown in Fig. 11. This means that they can be used with almost collinear writing beams, and therefore the depth-resolution is not compromised by walkoff as for bulk photorefractive crystals. The fabrication and operation of such MQW devices are described in [30] and [31].

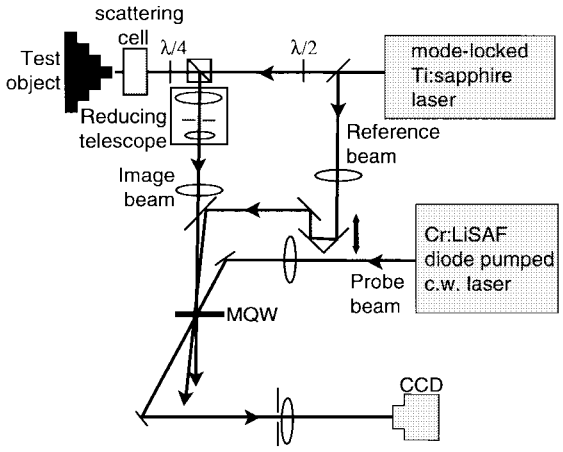

Fig. 12. Experimental configuration of the MQW holographic imaging system.

The MQW device reported here was used in the transverse Franz–Keldysh geometry. This requires a large applied voltage, of the order of 10 kV/cm, to be applied in the plane of the quantum wells, parallel to the optical grating vector being written. Photocarriers are preferentially excited in the bright regions and drift to shield the applied field in these regions. Consequently the net electric field varies with the

period of the light intensity fringe pattern. As with their bulk crystal counterparts this electric field modulation is mapped to a refractive index/absorption modulation using an electro-optic effect (here $\Delta n \propto E^2$ unlike the pockels effect used in most bulk photorefractives). The hologram fringe patterns are again therefore a record of the spatial variations in the incident optical field, rather than the absolute intensities.

The experimental apparatus shown in Fig. 12 was used to record and reconstruct depth-resolved holograms in the MQW devices using a mode-locked femtosecond Ti:sapphire laser. The polarization of the writing beams was perpendicular to the plane of the hologram. The object was imaged in reflection onto the MQW device. The reference and probe (i.e., readout) beam were both weakly focused using 0.5-m focal length lenses. In this experiment the writing beams were separated by an angle of 1.5°, corresponding to a grating period of 32 μm. A diode-pumped Cr:LiSAF CW laser [32], was used to provide a reconstruction (probe) beam to read out the holograms. This laser was tuned to the exciton peak wavelength ($\sim$850 nm) to maximize hologram diffraction efficiency [31]. The hologram was reconstructed in a transmission geometry, diffracting into multiple orders. The zeroth order, which contains no image information, was blocked using a spatial filter, and the $+1$ or -1 diffracted order imaged onto a standard CCD camera using a 200-mm focal length lens. For all the experiments with the MQW devices described here, the total incident illumination intensity was kept approximately constant at 1 mW/cm^2 in the signal beam and 1.25 mW/cm^2 in the reference beam. The intensity of the reconstruction beam was 1.25 mW/cm^2 and the voltage applied across the device aperture was between 1.5 and 2 kV.

The performance of this system was first evaluated without a scattering medium present. The transverse resolution was measured by imaging a USAF test-chart onto the MQW device. The test-chart image was reconstructed on the diffracted order with a transverse resolution of 50 μm. In order to sensitively detect low intensity images, background subtraction was used to remove the unwanted illumination on the CCD from light scattered from fixed inhomogeneities in the MQW device. The depth resolution of the reconstructed image was measured by imaging the same 3-D test object described above, i.e., a series of concentric aluminum cylinders with diameters from 1 to 5 mm and separated in depth by 100 μm. The different layers of the object could be individually imaged and rendered into a 3-D volume, as for the experiments with Rh:$BaTiO_3$ crystal. The depth resolution was measured by determining the range of delays of the reference arm over which a single step of the object remained visible and found to be $\sim$50 μm. This confirmed that walkoff was not compromising the spatial resolution

The MQW device was also used to image the test objects through a scattering solution. In these experiments a weak spatial filter (of 1-mm radius in the Fourier plane of a demagnifying telescope) was employed to remove stray surface reflections and also to reject some of the scattered light. The average power incident upon the scattered cell was about 2.8 W/cm^2. With a solution of 9-mfp scattering depth, the test-chart was completely obscured when imaged directly as shown in Fig. 13(a). However, in the reconstruction of the hologram recorded in the MQW device, the test-chart can be clearly seen with a transverse resolution of $\sim$50 μm [see Fig. 13(b)]. It was found that much of the speckle that is evident in this image could be removed by slightly vibrating one of the mirror mounts in the reference arm, thereby averaging the speckle over the integration time of the MQW device. A higher quality image obtained in this manner is shown in Fig. 13(c). The 3-D test object was then imaged through a scattering solution corresponding to 8 mfp (see Fig. 13). Directly imaged the object was totally obscured, but in the holographic reconstruction the layers of the object are clearly observable [see Fig. 14(a)–(c)]. The depth resolution was measured to be $\sim$50 μm. A computer generated reconstruction of the 3-D object is shown in Fig. 14(d).

(a) (b) (c)

Fig. 13. USAF test-chart (a) imaged directly through 9 mfp of scattering medium, (b) holographic reconstruction, (c) holographic reconstruction obtained when vibrating reference beam.

The response time of the MQW device was measured whilst imaging the 3-D object through the scattering medium (with experimental parameters stated above) by chopping the reference beam and synchronously detecting the diffracted image signal at the chopping frequency using a photodiode and a lock-in amplifier. When the chopping frequency became comparable to the response time, the grating formation in the MQW device could no longer follow the modulation and the lock-in signal decreased. This is represented in Fig. 15, which shows the variation in the lock-in amplifier signal as a function of modulation frequency. The grating formation in the MQW device appeared to follow the modulation for frequencies at least up to 2.5 kHz (limited by the maximum frequency of the mechanical chopper). This corresponds to a response time of $<$0.4 ms, which is well above normal video rate (30 frames per second) and so demonstrates real time image acquisition.

III. Conclusion

We have demonstrated the use of a photorefractive holographic imaging system as a coherence gate to discriminate against scattered light and provide depth resolved images through turbid media. We have discussed the performance of this ballistic imaging technique in terms of its spatial resolution, sensitivity, dynamic range, and image acquisition time. Using rhodium-doped barium titanate as the hologram recording medium, we have recorded depth-resolved images through turbid media of up to 16-mfp scattering depth with sub-100-μm depth and transverse spatial resolution. This has been achieved using a low-cost (4 b) CCD camera. We have established that our sensitivity is currently limited by the optical quality of our photorefractive crystals. The use of a more efficient photorefractive medium, or background

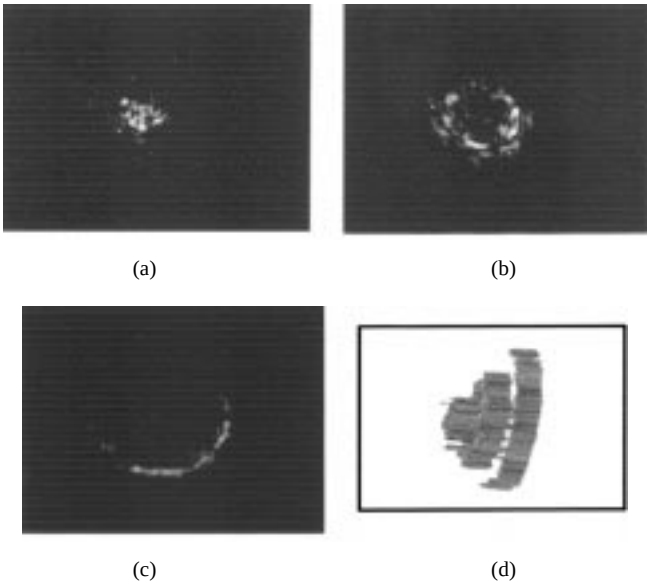

Fig. 14. Images of 3-D object through 8 mfp of scattering medium using MQW imaging system. (a)–(c) depth-resolved holographic images of 3-D object layers, (d) 3-D computer rendering from depth-resolved images.

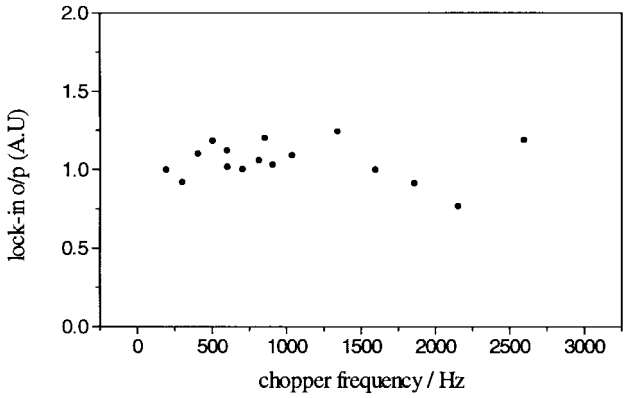

Fig. 15. The diffraction efficiency of a MQW device as a function of the modulation frequency of the imaging beam.

subtraction of the scattered read-out beam using a high-bit depth camera will increase the sensitivity and hence the imaging depth through turbid media.

For real world applications we require a system that has a faster response time than rhodium-doped barium titanate. There are other suitable candidates amongst the bulk photorefractive materials such as cadmium telluride, which will be the subject of further investigation. We have investigated the use of GaAs–AlGaAs semi-insulating MQW devices as the hologram recording medium and have demonstrated holographic imaging with transverse and depth resolution of $\sim$50 μm. We have used this system to acquire images with a transverse spatial resolution of 50 μm through a scattering medium of 9-mfp depth and have demonstrated 3-D imaging with a depth resolution of $\sim$50 μm through 8 mfp of scattering medium. The image acquisition time of the MQW devices has been measured to be less then 0.4 ms that is faster than normal video rate and therefore appropriate for "real time" imaging.

ACKNOWLEDGMENT

The authors gratefully acknowledge invaluable discussions with M. Klein, B. Wechsler, D. Rytz, and E. N. Leith.

REFERENCES

[1] R. Mellish, N. P. Barry, S. C. W. Hyde, R. Jones, P. M. W. French, J. R. Taylor, C. J. van der Poel, and A. Valster, "Diode-pumped Cr:LiSAF all-solid-state femtosecond oscillator and regenerative amplifier," *Opt. Lett.*, vol. 20, pp. 2312–2314, 1995.
[2] G. E. Anderson, F. Liu, and R. R. Alfano, "Microscope imaging through highly scattering media," *Opt. Lett.*, vol. 19, pp. 981–983, 1994.
[3] D. S. Dilworth, E. N. Leith, and J. L. Lopez, "Three-dimensional confocal imaging of objects embedded within thick diffusing media," *Appl. Opt.*, vol. 30, pp. 1796–1803, 1991.
[4] B. B. Das, K. M. Yoo, and R. R. Alfano, "Ultrafast time-gated imaging in thick tissues: A step toward optical mammography," *Opt. Lett.*, vol. 18, pp. 1092–1094, 1993.
[5] K. M. Yoo, Q. R. Xing, and R. R. Alfano, "Imaging objects in highly scattering media using femtosecond second harmonic generation cross correlation time-gating," *Opt. Lett.*, vol. 16, pp. 1019–1021, 1991.
[6] J. A. Moon, R. Mahon, M. D. Duncan, and J. Reintjes, "Three-dimensional reflective image reconstruction through a scattering medium based on time-gated Raman amplification," *Opt. Lett.*, vol. 19, pp. 1234–1236, 1994.
[7] M. R. Hee, J. A. Izatt, E. A. Swanson, and J. G. Fujimoto, "Femtosecond transillumination tomography in thick tissues," *Opt. Lett.*, vol. 18, pp. 1107–1109, 1993.
[8] H. Chen, Y. Chen, D. Dilworth, E. Leith, J. Lopez, and J. Valdmanis, "Two-dimensional imaging through diffusing media using 150-fs gated electronic holography techniques," *Opt. Lett.*, vol. 16, pp. 487–489, 1991.
[9] M. P. Rowe, E. N. Pugh Jr., J. S. Tyo, and E. Engheta, "Polarization-difference imaging: A biologically inspired technique for observation through scattering media," *Opt. Lett.*, vol. 20, pp. 608–610, 1995.
[10] J. Watson, P. Georges, T. Lepine, B. Alonzi, and A. Brun, "Imaging in diffuse media with ultrafast degenerate optical parametric amplification," *Opt. Lett.*, vol. 20, pp. 231–233, 1995.
[11] M. R. Hee, J. A. Izatt, J. M. Jacobson, J. G. Fujimoto, and E. Swanson, "Femtosecond transillumination optical coherence tomography," *Opt. Lett.*, vol. 18, pp. 950–952, 1993.
[12] A. V. Mamaev, L. I. Ivleva, N. M. Polozkov, and V. V. Shkunov, "Photorefractive visualization through opaque scattering media," *Conf. Lasers and Electro-Optics*, paper CFK6, 1993, pp. 632–634.
[13] A. Knuttel, J. M. Schmitt, and J. R. Knutson, "Low-coherence reflectometry for stationary lateral and depth profiling with acousto-optic deflectors and a CCD camera," *Opt. Lett.*, vol. 19, pp. 302–304, 1994.
[14] D. Huang, E. A. Swanson, C. P. Lin, J. S. Schuman, W. G. Stinson, M. R. Hee, T. Flotte, K. Gregory, C. A. Puliafito, and J. G. Fujimoto, "Optical coherence tomography," *Science*, vol. 254, pp. 1178–1181, 1991.
[15] N. Abramson, "Light-in-flight recording by holography," *Opt. Lett.*, vol. 3, pp. 121–123, 1978.
[16] A. Rebane and J. Feinberg "Time-resolved holography," *Nature*, vol. 351, pp. 378, 1991.
[17] A. Ishimaru, *Wave Propagation and Scattering in Random Media*, Academic Press Inc., vol. 1, 1978.
[18] P. Gunter and J. P. Huignard Eds., *Photorefractive Materials and their Applications Vol. I*, Topics in Applied Physics. Berlin, Germany: Springer-Verlag, 1988.
[19] E. Leith, C. Chen, H. Chen, Y. Chen, D. Dilworth, J. Lopez, J. Rudd, P.-C. Sun, J. Valdmanis, and G. Vossler, "Imaging through scattering media with holography," *J. Opt. Soc. Amer. A*, vol. 9, pp. 1148–1153, 1992.
[20] E. N. Leith, C. Chen, H. Chen, Y. Chen, J. Lopez, P.-C. Sun, and D. Dilworth, "Imaging through scattering media using spatial incoherence techniques," *Opt. Lett.*, vol. 16, pp. 1820–1822, 1991.
[21] K. G. Spears, J. Serafin, N. Abramson, X. Zhu, and H. Bjelkhagen, "Chrono-coherent imaging for medicine," *IEEE Trans. Biomed. Eng.*, vol. 36, pp. 1210–1231, 1989.
[22] S. C. W. Hyde, N. P. Barry, R. Jones, J. C. Dainty, P. M. W. French, M. B. Klein, and B. A. Wechsler, "Depth-resolved holographic imaging through scattering media using photorefraction," *Opt. Lett.*, vol. 20, pp. 1331–1333, 1995.
[23] H. Kogelnik, "Coupled wave theory for thick hologram gratings," *Bell Syst. Tech. J.*, vol. 48, pp. 2909–2947, 1969.

[24] J. E. Ford, Y. Fainman, and S. H. Lee, "Enhanced photorefractive performance from 45°-cut barium titanate," *Appl. Opt.*, vol. 28, pp. 4808–4815, 1989.
[25] S. C. W. Hyde, N. P. Barry, R. Jones, J. C. Dainty, and P. M. W. French, "Sub 100 mm depth resolved holographic imaging through scattering media in the near infrared," *Opt. Lett.*, vol. 20, pp. 2330–2332, 1996.
[26] R. Jones, S. C. W. Hyde, M. J. Lynn, N. P. Barry, J. C. Dainty, P. M. W. French, K. M. Kwolek, D. D. Nolte, and M. R. Melloch, "Holographic storage and high background imaging using photorefractive multiple quantum wells," *Appl. Phys. Lett.*, vol. 69 pp. 1837–1839, 1996.
[27] D. D. Nolte, D. H. Olson, G. E. Doran, W. H. Knox, and A. M. Glass, "Resonant photodiffractive effect in semi-insulating multiple quantum wells," *J. Opt. Soc. Amer. B*, vol. 7, pp. 2217–2225, 1990.
[28] Q. Wang, R. M. Brubacker, D. D. Nolte, and M. R. Melloch, "Photorefractive quantum wells: Transverse Franz–Keldysh geometry," *J. Opt. Soc. Amer. B*, vol. 9, pp. 1626–1641, 1992.
[29] D. A. B. Miller, D. S. Chemla, and T. C. Damen, "Band-edge electroabsorption in quantum well structures: The quantum confined stark effect," *Phys. Rev. Lett.*, vol. 53, pp. 2173–2176, 1984.
[30] K. M. Kwolek, M. R. Melloch, and D. D. Nolte, "Dynamic holography in a reflection/transmission photorefractive quantum-well asymmetric Fabry-Perot," *Appl. Phys. Lett.*, vol. 65, pp. 385–287, 1994.
[31] D. D. Nolte and K. M. Kwolek, "Diffraction from a short cavity Fabry-Perot—Application to photorefractive quantum wells," *Opt. Comm.*, vol. 115, pp. 606–616, 1995.
[32] R. Mellish, P. M. W. French, J. R. Taylor, P. J. Delfyette, and L. T. Florez, "All solid-state femtosecond diode pumped Cr:LiSAF laser," *Electron. Lett.*, vol. 30, pp. 1262–1263, 1994.

Sam C. W. Hyde was born in Welwyn Garden City, U.K., in 1972. He received the B.Sc. degree in physics in 1993 and the Ph.D. degree in biomedical imaging and ultrafast lasers in 1997 from Imperial College of London University.

He is currently employed as a Research Assistant in the Femtosecond Optics Group in the Physics Department at Imperial College. His research interests include photorefractive imaging, flourescence lifetime imaging and diode-pumped ultrafast solid-state lasers and amplifiers.

Dr. Hyde is a member of the Institute of Physics and the Optical Society of America.

Richard Jones was born in Wrescam, U.K., in 1972. He received the B.Sc. degree in Physics from Imperial College of London University in 1993 and the M.Sc. degree in optoelectronics and microwaves from University College, London University, in 1994. He is currently working toward the Ph.D. degree in diode-pumped laser technology and the application of photorefractives for medical imaging in the Physics Department at Imperial College.

Mr. Jones is a member of the Institute of Physics an dof the Society of Photo-Optical Instrumentation Engineers.

Nick P. Barry was born in Portsmouth, U.K., in 1963. He received the B.Sc. degree in medical physics from Queen Elizabeth College, London University, in 1984, and the M.Sc. degree in applied and modern optics from the University of Reading, U.K., in 1989. He received the Ph.D. degree from Imperial College, London University, in 1996.

He is currently employed as a Research Assistant in the Femtosecond Optics Group in the Physics Department at Imperial College, London University. His research interests include photorefractive materials, diode-pumped laser technology, and applications to biomedical imaging.

Dr. Barry is a member of the Optical Society of America.

J. C. Dainty (M'83) was born in Ontario, Canada, in 1947. He received the Ph.D. degree from Imperial College, London University, in 1972.

He was a Lecturer at Queen Elizabeth College, London University, from 1974 to 1978, Associate Professor at the Institute of Optics, University of Rochester, NY, from 1978 to 1983, and is currently Pilkington Professor of Applied Optics at Imperial College. His research interests include imaging through turbulent and scattering media and electromagnetic aspects of scattering and imaging.

Prof. Dainty was awarded the ICO Prize in 1984 and the Thomas Young Medal and Prize from the U.K. Institute of Physics in 1994. He was President of the International Commission for Optics from 1990 to 1993 and is currently an Editor of the journal *Optics Communications*. He is a Fellow of the Institute of Physics, of the Society of Photo-Optical Instrumentation Engineers, and of the Optical Society of America. He is a member of the Royal Astronomical Society.

Paul M. W. French was born in Felixstowe, U.K., on January 27, 1962. He received the B.Sc. degree in physics and the Ph.D. degree for work on femtosecond dye lasers, both from Imperial College, London University. in 1983 and 1987, respectively.

In 1990 to 1991 he worked on ultrafast all-optical switching in optical fibers as a Consultant at AT&T Bell Laboratories in Holmdel, NJ. He is currently a Lecturer in the Physics Department of Imperial College, where he has researched generation and application of ultrashort optical pulses. His current research interests include the development of compact all-solid-state turnable/ultrafast lasers and their applications to biomedical imaging and other instrumentation.

Dr. French is a member of the Institute of Physics and the Optical Society of America.

K. M. Kwolek was born in Wallingford, CT, in March 1970. She received the B.S. degree in physics from Rensselear Polytechnic Institute, Troy, NY, in 1992, and the M.S. degree in physics from Purdue University, West Lafayette, IN, in 1994. She is currently pursuing the Ph.D. degree at Purdue.

Her research interests include the enhancement of photorefractive thin film diffractive performance.

Ms. Kwolek is a member of the Optical Society of America.

David D. Nolte was born in Akron, OH, on January 30, 1959. He received the bachelor's degree in physics from Cornell University in 1981 and the Ph.D. degree from the University of California at Berkeley in 1988.

His doctoral research led to the first experimental measurement of bandedge hydrostatic deformation potentials in semiconductors using the concept of internal reference levels. In September 1988, he joined Bell Laboratories as a Post-Doctoral Member of the Technical Staff. He joined the faculty of physics at Purdue University, West Lafayette, IN, in 1989, and was promoted to Associate Professor in 1994. His research interests include ultra-low-density nonlinear optics, optoelectric properties, and applications of semi-insulating semiconductor heterstructures, magnetic phenomena in electro-optics and nonlinear optics, and the physics of mesoscopic point-like defects in semiconductors.

M. R. Melloch (S'76–M'76–SM'91), photograph and biography not available at the time of publication.